

A NEW APPROACH FOR EVALUATING RADIATION EMBRITTLEMENT OF REACTOR PRESSURE VESSEL STEELS

J. A. Wang and N. S. V. Rao
Oak Ridge National Laboratory
Oak Ridge, TN 37831-6171
wangja@ornl.gov, raons@ornl.gov

ABSTRACT

A new approach is developed to predict the radiation embrittlement of reactor pressure vessel steels. The Charpy transition temperature shift data contained in the Power Reactor Embrittlement Database is used in this study. The results indicate that this new embrittlement predictor achieved about 67.3% and 52.4% reductions respectively, in the uncertainties for General Electric (GE) Boiling Water Reactor plate and weld data compared to Regulatory Guide 1.99, Rev. 2 (RG1.99/R2). The implications of irradiation temperature effects for the development of radiation embrittlement models are then discussed. A new approach for the Charpy trend curve is also developed, which incorporates the chemical compositions into the governing fitting equation. This approach reduces the uncertainty of Charpy data fitting and provides an expedient scheme to link and project the surveillance test results to those for reactor pressure vessel steels.

Keywords—radiation embrittlement, reactor vessel integrity, information fusion, power reactor, boiling water reactor, material modeling, Charpy curve fitting

INTRODUCTION

The aging and degradation of light-water reactor pressure vessels (RPVs) are of particular concern because the magnitude of the radiation embrittlement is extremely important to the plant's safety and operating cost. Property changes in materials due to neutron-induced displacement damage are a function of neutron flux, neutron energy, and temperature — as well as the pre-irradiation material history, material chemical composition, and microstructure — since each of these influence radiation-induced microstructural evolution. These factors must be considered to reliably predict RPV embrittlement and to ensure the structural integrity of the RPV. Based on the embrittlement predictions, decisions must be made concerning operating parameters, low-leakage-fuel management, possible life extension, and the potential role of pressure vessel annealing. Therefore, the development of embrittlement prediction models for nuclear power plants (NPPs) is a very important issue for the nuclear industry regarding the safety and lifetime extension of aging commercial nuclear power plants.

The general degradation mechanisms of material aging behavior can be quite complicated. They include microstructure and compositional changes, time-dependent deformation and resultant damage accumulation, environmental attack and the accelerating effects of elevated temperature, and synergistic effects of all the above. These complex nonlinear dependencies make the modeling of aging material behaviors a difficult task. There have been several domain (mechanism) models that capture various aspects of material behavior; these models are designed by the domain experts to capture various critical relationships. At the same time, conventional nonlinear estimators — while requiring very limited domain expertise — can model relationships that are not readily apparent. Consequently, there has been a profusion of methods with complementary performance, and no single method has proved to be always better than all others. Our goal is to develop an effective methodology by combining the domain models with the nonlinear estimators, including neural networks and NNRs (NNR) to exploit their complementary strengths.

We have previously developed a large Power Reactor Embrittlement Database (PR-EDB) [1] for U.S. nuclear power plants. Subsequently, in cooperation with the Electric Power Research Institute, additional verification and quality assurance of the data was performed by the U. S. reactor vendors. PR-EDB is used in this study to predict the embrittlement levels in light-water RPVs. The results from a newly developed near neighbor projective fuser indicate that our combined predictor achieved about 67.3% and 52.4% reductions, respectively, in the embrittlement uncertainties for the GE Boiling Water Reactor plate and weld data compared to RG1.99/R2.

A new methodology that incorporates the chemical compositions into the Charpy trend curve was also developed. The purpose of this new fitting procedure is to generate a new multi-space topography that can properly reflect the inhomogeneity of the surveillance materials and utilize this multi-space trend surface to link and project the surveillance test results to that those for RPV steels.

The Trend Curve Development for Charpy Impact Data

Ferritic RPV materials undergo a transition in fracture behavior from brittle to ductile as the test temperature of the material is increased. Charpy V-notch impact tests are conducted in the nuclear industry to monitor changes in the

fracture behavior during power reactor service. Neutron irradiation to a certain threshold causes an upward shift in the ductile-to-brittle transition (DBTT) and a drop in the upper shelf energy. The nuclear industry indexes the DBTT at 30 ft-lbs (41J) of absorbed energy, and the shift in the DBTT is referred as ΔRT_{NDT} or ΔT_{30} . This transition temperature shift data is also used as the primary index of RPV embrittlement for this study.

In general, in order to obtain the ΔRT_{NDT} or ΔT_{30} , the raw Charpy impact test data, including unirradiated and irradiated data sets, need to be fit through a data fitting procedure to develop appropriate trend curves. The current practice of Charpy curve-fitting procedures used in PR-EDB is based on the hyperbolic tangent model [2], which has been proven to be successful for the determination of transition temperature for materials that have more or less homogeneous properties. The impact energy and testing temperature are used as the two primary input parameters for the determination of the fitting curve. The hyperbolic tangent model relates impact energy E to the test temperature T according to Equation 1:

$$E = \left(\frac{USE + LSE}{2} \right) + \left(\frac{USE - LSE}{2} \right) * \text{Tanh}(\text{SLOPE} * (T - T_M)) \quad (1)$$

with USE and LSE as the upper- and lower-shelf energy, respectively, with T_M as the midpoint of the transition temperature region, and $SLOPE$ as the slope of the curve at T_M . This model is purely phenomenological but characterizes the general shape of a Charpy curve well in terms of the four basic parameters, USE , LSE , T_M , and $SLOPE$. The hyperbolic tangent function is the most widely used fitting procedure next to hand (eyeball) fitting.

For a particular raw Charpy data set provided with chemistry information for each individual specimen, if certain data exhibit a large degree of scatter about the best-fit line, detailed study from PR-EDB [1] shows that these data generally either have a much higher or lower Cu content than the rest of the specimens. This was illustrated in Fig. 1 with weld data from capsule T of Zion Unit 2, where the Charpy data with the lowest Cu content at 0.12 wt% have the highest impact energy, 119 Joule. This may imply that when the greater inhomogeneity of specific test sets is known, further constraints need to be added into the Charpy curve-fitting model, such as Cu and Ni contents, to reduce the uncertainty and to reflect the inhomogeneity or chemical variability of the tested surveillance materials. Furthermore, the surrogate materials, especially for many weld

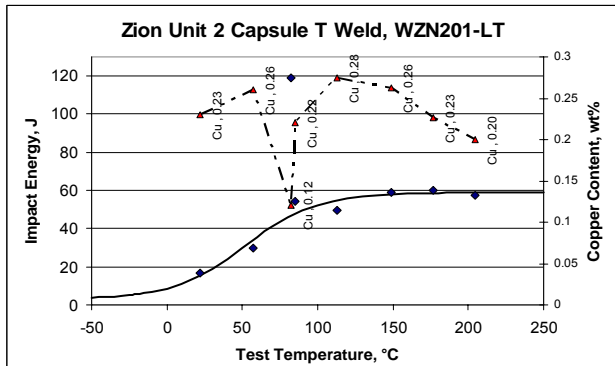


FIG. 1—Chemical variability of Charpy data.

materials of the RPV beltline, were used in the U.S. power reactor RPV surveillance program. Thus, developing a proper procedure to cope with the chemistry variability may directly provide a bridge and proper safety margin in linking the radiation embrittlement of the surveillance test samples to that of the RPV beltline materials.

Proposed New Fitting Function with Consideration of the Chemistry Variability

In order to consider the chemical variability of the surveillance test samples, a new fitting procedure that incorporates the chemical composition into the governing equation was developed. The formula for the impact energy as a function of test temperature (T), and Cu and Ni (plus other chemistry, such as P, Mn, etc.) can be written as:

$$E = \left\{ A + B * \text{Tanh} \left[\frac{T - T_M}{C} \right] \right\} * f(Cu, Ni, \dots) \quad (2)$$

The preliminary testing function of function f , for Cu and Ni contents, can be written as follows:

$$f(Cu, Ni) = C_5 * Cu + C_6 + C_7 * \sqrt{Cu * Ni} \quad (3)$$

where $A=(USE+LSE)/2$, $B=(USE-LSE)/2$, $C=1/SLOPE$, and C_i are constant fitting parameters. This approach assumes that there is no major change of the general trend between the new fitting equation and the conventional fitting curve without the consideration of chemical variability.

This new fitting procedure provides a new multi-dimension topography that can properly reflect the inhomogeneity of the surveillance materials.

Advanced Charpy Data Fitting Function

A physical shape of the hyperbolic tangent fit function for a Charpy test set is dictated by the USE , LSE , and midpoint temperature at the transition region, T_M , and the slope at the T_M as described in Equation 1. The new fitting approach as presented in Equation 2 can only scale the impact energy up or down without significantly changing the overall shape of the trend curve, such as the slope and temperature range at the middle point of the transition region. In order to have more freedom in adjusting the hyperbolic tangent fit curve, a more sophisticated formulation of the proposed new fitting procedure that takes into account the shape change of the hyperbolic tangent fit curve was developed and is illustrated in Equation 4:

$$E = \left\{ A + B * \text{Tanh} \left[\frac{T - T_0 / f_1}{C * / f_2} \right] \right\} * f_3 + f_4 \quad (4)$$

where, f_i , $i=1,4$, are functions of chemical compositions for Cu and Ni contents, which are written as follows,

$$f_1 = C_8 * Cu, \quad f_2 = C_9 * Cu, \quad f_3 = C_{10} * (Cu * Ni) + C_{11} \quad (5)$$

$$f_4 = C_5 * C + C_6 * \sqrt{Cu * Ni} + C_7$$

where C_i , $i=5, 11$ are constant-fitting parameters.

The function f_1 to f_4 was introduced in the advanced data fitting function as described in Equation 4, where the f_1 is used to adjust temperature range at the middle point, f_2 is used

to adjust the slope at the middle point, f_3 is used to scale the impact energy curve up or down, and f_4 is used to adjust the fitting bias.

However, the authors would like to mention that to use the proposed formula, the user needs to have enough data to avoid overfitting phenomena. If there are not sufficient data, the user needs to consider reducing the number of the suggested fitting parameters.

Results of the Proposed Fitting Procedures

The weld Charpy data, with HEAT_ID = WDR301 listed in PR-EDB, from surveillance capsule 18 of Dresden Unit 3 nuclear power plant were used for this feasibility study. The mean chemistry of the Charpy set for Cu and Ni contents is 0.2077 and 0.353 wt% respectively.

Conventional Hyperbolic Tangent Fit Result — Equation 1 was used in the curve fitting, where IMSL routine ZXSSQ was used in the nonlinear least squares fitting evaluation to determine the constant fitting parameters. Based on Equation 1, the estimated one standard deviation is 13.84°C for the selected WDR301 surveillance data set. The estimated constant-fitting parameters are A=50.85 J, B= 47.85 J, $T_M=15^\circ\text{C}$, and SLOPE = 0.0179. The corresponding hyperbolic tangent fitting curve and data are shown in Fig. 1a.

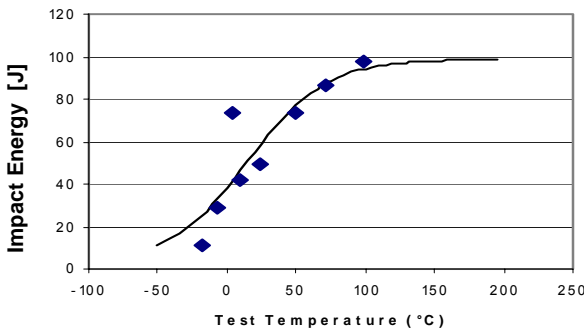


FIG. 1a—Charpy data of Dresden Unit3 Capsule 18 WDR301 in TL orientation.

New Fitting Function Test Results — A FORTRAN program was written for this feasibility study, where IMSL routine ZXSSQ was used in the non-linear least squares fitting. Based on Equation 2, the estimated one standard deviation is 12.09°C. The estimated constant-parameters are listed below. A= 50.85 J, B=47.85 J, $T_M=8.0^\circ\text{C}$, and SLOPE = 0.0379, C5 =15.09, C6=2.869, and C7=-18.5.

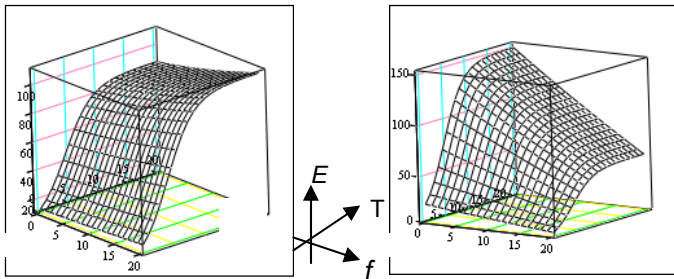


FIG. 2—3-D plot of Eq. 2, with Ni fixed at average 0.353 wt %.

FIG. 3—3-D plot of Eq. 2 with Cu fixed at average 0.2077 wt %.

Advanced Testing Function Fit Results — Based on Equation 4, the estimated one standard deviation is 10.05°C. The estimated constant-parameters are listed below.

A=50.3 J, B=47.3 J, $T_0=5.87^\circ\text{C}$, and SLOPE = 0.00805, C5 =1032, C6=-123, C7=-277.4, C8=1.566, C9=1.987, C10=-25.47, and C11=2.891. Because only eight data points were available in this modeling fitting development, no training and testing set data were assigned. The examination of the overfitting phenomena was done by evaluating the 3-D plots to see any anomaly or self-inconsistency, as shown in Figs 4 and 5. It appears from the plots that the generated topology is still very closely followed the hyperbolic tangent characteristic of the Charpy impact test data. No obvious overfitting can be identified, this may be partially due to the hyperbolic tangent constraint assigned in the Equation 4.

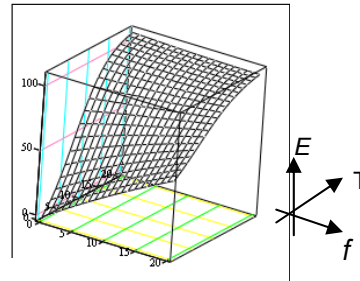


FIG. 4—3-D plot of Eq. 3, with Ni fixed at average, 0.353 wt %.

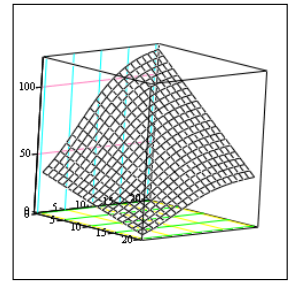


FIG. 5—3-D plot of Eq. 3 with Cu fixed at average, 0.2077 wt %.

Applying New Fitting Procedure for Surrogate Material Research

Based on the proposed new fitting procedure, a multi-dimension topography can be generated. For simplification, the 3-D Cartesian coordinate is used to illustrate the developed multi-dimension topography (see Fig. 6), where test temperature and impact energy stand for the x and z coordinates, respectively, and the third axis represents the integrated formulation of the chemistry composition functions, f_i .

Evaluation of the Trend Curve for the Target Chemistry Data — Based on constructed multi-space topography, as illustrated in Fig. 6, one can substitute the target chemistry into a new Charpy fitting equation and develop a new trend curve for

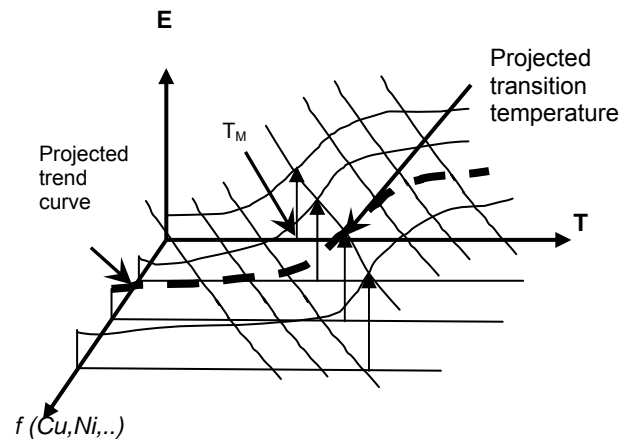


FIG. 6—Illustration of projected trend curve.

the target materials. Therefore, this new procedure provides an expedient way to determine the trend curve for the surrogate materials of the RPV surveillance program. Furthermore, based on this new approach, the new advanced fitting procedure achieves a reduction in uncertainty by 27%, compared to that of the conventional hyperbolic tangent fit procedure. However, caution should be exercised while using these fitting functions, because of high-order nonlinearity, and the chemistry of the target materials should be within one standard deviation of the mean chemistry from which the new fitting equation was developed.

New Approach for Evaluating Radiation Embrittlement

Background

The complex nonlinear dependencies observed in typical material aging data, as well as the existence of large uncertainties and data scatter, make nonlinear material behavior prediction a difficult task. The conventional statistical and deterministic approaches have proven to result in large uncertainties, in part because they do not fully exploit the domain specific knowledge. The domain models built by researchers in the field, on the other hand, cannot fully exploit the statistical and information content of the data. As evidenced in previous studies, it is unlikely that a *single* method, whether it is statistical, nonlinear, or domain model, will outperform all others. Considering the complexity of the problem, it is more likely that certain methods will perform best under certain conditions. In this paper, we propose to combine a number of methods such as domain models, neural networks, and NNRs. Such a combination of methods became possible because of recent developments in measurement-based optimal fusers [3-5] in the area of information fusion.

The problem of estimating nonlinear relationships from noisy data has been well studied in the area of statistical estimation [6]. The nonlinear statistical estimators such as the Nadaraya-Watson estimator and regressograms [7] essentially rely on the properties of regressions. While neural networks and statistical estimators are general, the domain models developed by the material scientists specifically capture the critical relationships in the data that are not easily amenable to general methods. Such models are typically based on a combination of linear and nonlinear models, which are carefully chosen through an understanding of experimental data.

Information Fusion Approach

Particularly among the models developed for embrittlement data, there is unlikely to be a single winner, and different models perform well under different conditions. By discarding one or more models, one stands the risk of not characterizing certain critical performance. We propose to combine various methods using the isolation fusers discussed in [6]. The most important part of these fusers is that the combined system can be guaranteed to be at least as good, according to a chosen criterion such as prediction error, as the best individual estimator with a specified probability. Informally, the isolation property ensures that the fuser is at least capable of simply imitating any of the sensors, but in general can perform much better. This result is distribution-free in that no assumptions are

made on the underlying error distributions; as a result, the guarantee is with a probability that approaches 1 as data size approaches infinity. Furthermore, for finite data sets, this probability can be computed based on the sample size; or, given the probability the required sample size can be computed. In practice, however, the sample size estimates are typically larger than the minimum required for a specific application at hand. This is to be expected since the sample size estimates are distribution-free and are valid for a broad class of applications. Furthermore, fusion of no proper subset of the models performs better than the fused system based on all models. Thus, the positive aspects of *all* individual estimators can be exploited without discarding any single estimator. The deployment of these fusers on various models will ensure (probabilistically) that the fused model is at least as good as the best of the individual models, irrespective of their individual performances. However, because of the general nature of the results on fusers, the actual performance gains in a particular application are often better than the guarantees. For example, the required sample size could be much smaller (but never larger) than the predicted sample size. We show here that significant performance improvements are indeed obtained by employing fusers to combine various embrittlement models.

Methodology Used for Developing Embrittlement Models

We employ neural networks, NNRs, and domain models, based on the PR-EDB data, to predict the Charpy transition temperature shift (ΔT_{30}) of RPV materials. From past experience [8], the boiling water reactor (BWR) data has larger uncertainty than the other power reactor data. In this study, we focused only on the BWR data.

The first task is to create unbiased training and test sets. The GE BWR surveillance data (listed in PR-EDB) were preprocessed and streamlined, and the one-to-one data relationship was constructed. The GE BWR data values were then scaled to the interval [-1, 1] using a linear max/min transformation. This ensures that no one component in the data dominates the parameter optimization scheme. Then the data were randomly partitioned into training and testing sets. The GE BWR data (112 samples) were used in the study: they included 64 surveillance base data where 54 data were used as a training set and 10 data were used as a testing set, and 48 surveillance weld data where 40 data were used as a training set and 8 data were used as a testing set. The sensitivity of the sample size was not investigated in the current study.

The second task consists of determining a number of estimators for this problem. For each method, a criteria function and optimization routine will be selected that consistently produces stable results. For statistical estimators, we will follow the procedure described in the literature. For artificial neural networks (ANN), one hidden layer and eleven hidden nodes were chosen with 2000 epoch iteration. A random generator was used to generate the initial weights for ANN modeling. Four sets of ANN models were tested. We then combined the statistical and deterministic estimators using information fusion techniques.

An optimal projective fuser [4] proposed earlier was based on the lower envelope of error regressions of the estimators. In most practical cases, however, the error regressions are not available and only a finite sample is given. Consequently, this fuser is hard to implement and furthermore provides only asymptotic consistency. In this paper, we propose a projective

fuser based on the nearest neighbor concept [9], which is easy to implement. The combined system is guaranteed to perform at least as well as the best of the constituents by exploiting the regions where the individual methods are superior.

A novel methodology is developed here for inferring nonlinear relationships that are typical in material behavior prediction. A tool based on this methodology is also implemented for the embrittlement prediction of NPPs. This tool could be expanded and adapted for use in other areas in which nonlinear material properties are important, such as failure analysis of an earthquake event, airplane safety analyses, and others.

Embrittlement Prediction Models

In this section we briefly describe various models used for embrittlement prediction, which will be combined in the next section.

Oak Ridge National Laboratory (ORNL) Embrittlement Prediction Models — The residual defects in materials due to neutron induced-displacement damage are a function of neutron energy, neutron flux, exposure temperature, and the material properties that determine how neutrons interact with atoms and how defects interact within the material [10]. Thus, temperature, neutron flux, neutron energy spectrum, and material composition and processing history all contribute to the radiation embrittlement process [11]. Insufficient consideration of these factors may result in misleading correlations and, thus, incorrect predictions of material state and material behavior, as well as incorrect end-of-life determinations.

The development of new embrittlement prediction equations [8,12] stems from a series of studies on radiation embrittlement models, such as Guthrie's model [13], Odette's model [14], Fisher's model [15], B&W Lowe's model [16], the French FIM model [17], and several other parameter studies on the PR-EDB. Although the copper-precipitation model has been extremely successful in explaining many aspects of irradiation embrittlement, it is becoming increasingly evident that other elements also contribute to the embrittlement of RPV steel, such as Ni, P, Mn, Mo, and S. Theoretically, all the impurities in low-alloy steel are candidates to be included in the modeling. For example, C, Si, Mn, Mo, S, etc., were investigated in the test run, but including or excluding these elements did not affect the overall outcome of the statistical parameters significantly; therefore, these parameters (or elements) were not incorporated into final governing equations. Thus, Cu, Ni, and P were tentatively selected as key elements and were incorporated into the formula of the new prediction equations. Furthermore, the reason for separating weld and base metals is because the welds tend to show enhanced degradation, the welding process presents a possible region of physical and metallurgical discontinuity, and it offers added chances for the introduction of defects and undesirable components or stresses.

A nonlinear-least-squares fitting Fortran program was written for this study. The development of the parameters for this new embrittlement model is based on statistical formulation chosen by computer iterations. To some extent, the physical mechanisms are embedded in the equations, such as the formulation of the fluence factor. Two new prediction models for the GE BWR data were developed, where the fluence rate effect was considered in the second prediction model and are described below.

Model 1:

$$\begin{aligned} \Delta T (Base) &= [-94.8 + 411.9Cu + 247.3\sqrt{CuNi} + 498P/Cu]^* \\ & f^{0.3216 - 0.001003 \ln f} \quad (6) \\ \Delta T (Weld) &= [420.9Cu + 134.6\sqrt{CuNi} - 25.94P/Cu]^* \\ & f^{0.2478 - 0.01475 \ln f} \end{aligned}$$

Model 2

$$\begin{aligned} \Delta T (Base) &= \left[(13.62 + 318.1Cu - 58.75\sqrt{NiCu} - 151.4P/Cu)^* \right] \\ & f^{-0.4354 - 0.1285 \ln f} \\ & + \left[(18.44 - 49.13\sqrt{CuNi} - 17.22Cu - 97.57P/Cu)^* \right] \\ & f * (-8.344 - 0.7045 \ln f) * \ln(t_i / 600000) \quad (7) \\ \Delta T (Weld) &= 1.075 \left[(1580Cu - 86.06\sqrt{NiCu} + 43.55P/Cu)^* \right] \\ & f^{0.6523 + 0.02866 \ln f} \\ & - 2.23 \left[(4.193Ni - 45.54Cu)^* \right] \\ & f * (-11.63 - 0.4554 \ln f) * \ln(t_i / 600000) \end{aligned}$$

where ΔT is the transition temperature shift in °F; neutron fluence f is in units of 10^{19} n/cm² ($E > 1$ MeV); effective full power time, t_i , is in hours, and Cu, Ni, P are in wt%. The residuals, defined as "measured shift minus predicted shift," for ORNL Model 2 are illustrated in Figs. 7 and 8 for base and weld, respectively.

Regulatory Guide 1.99, Rev. 2 Model — The transition temperature shift of the RG1.99/R2 model [18] was also used in this study for comparison. It is described as follows.

$$\Delta RT_{NDT} = (CF) f^{(0.28 - 0.10 \log f)} \quad (8)$$

where, ΔRT_{NDT} is the transition temperature shift in °F, $CF(°F)$ is the chemistry factor (given in the Table 1 and Table 2 of RG1.99/R2), which is a function of Cu and Ni content, and neutron fluence f is in units of 10^{19} n/cm² ($E > 1$ MeV). The residuals for the RG1.99/R2 model are illustrated in Figs. 9 and 10 for base and weld, respectively.

Eason's Models — The developed embrittlement model by E. D. Eason et al. (Eason's model) [19] was used in this study. The Eason's trend curve of transition temperature shift was developed based on the power reactor data and is described in Equation 9. The residual of Eason's model is illustrated in Figs. 11 and 12 for base and weld, respectively.

$$\begin{aligned} \Delta T_{30p} &= ff_1(\phi t) + ff_2(\phi t) f(cc), \quad [°F] \\ ff_1(\phi t) &= A \cdot \exp \left[\frac{1.906 \cdot 10^4}{T_c + 460} \right] (I + 57.7 P) \left[\frac{\phi t}{10^{19}} \right]^a \\ ff_2(\phi t) &= \frac{1}{2} + \frac{1}{2} \tanh \left[\frac{\log(\phi t + 5.48 \cdot 10^{12} t_i) - 18.29}{0.600} \right] \\ ff(cc) &= B (Cu - 0.72)^{0.682} (I + 2.56 Ni^{1.358}) \quad (9) \end{aligned}$$

where, $a = 0.4449 + 0.0597 \cdot \log \left[\frac{\phi t}{10^{19}} \right]$, ϕt = fluence

Welds : $A = 1.10 \cdot 10^{-7}$, $B = 209$,
Plates : $A = 1.24 \cdot 10^{-7}$, $B = 172$
Forgings : $A = 0.90 \cdot 10^{-7}$, $B = 135$,
 T_c is coolant inlet temperature, °F

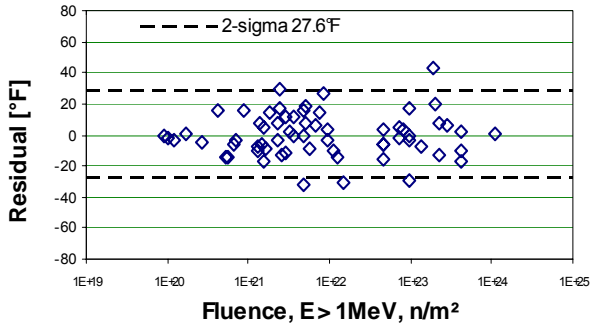


FIG. 7—ORNL Model 2 base residuals.

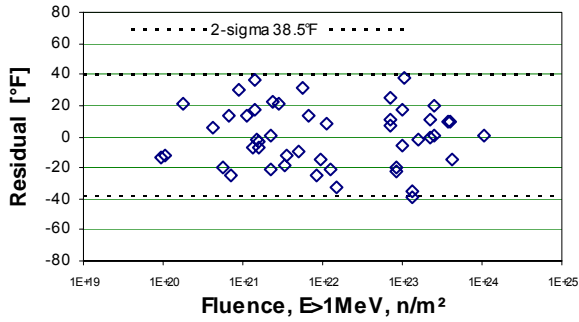


FIG. 8—ORNL Model 2 weld residuals.

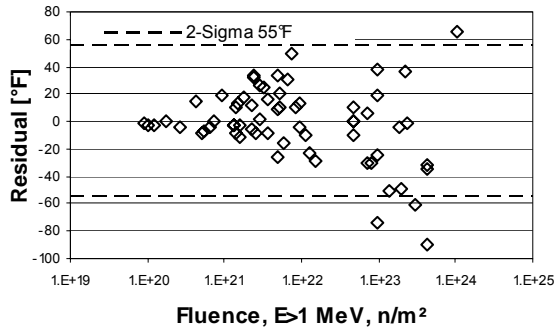


FIG. 9—R.G. 199/R2 base residuals.

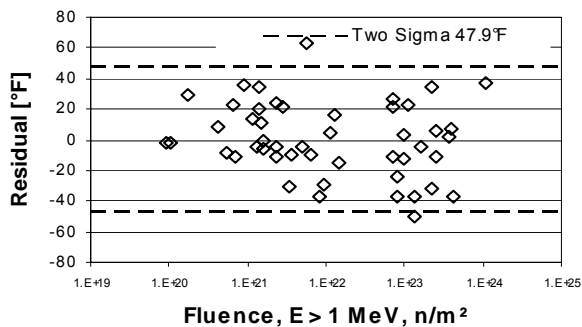


FIG. 10—R.G. 199/R2 weld residuals.

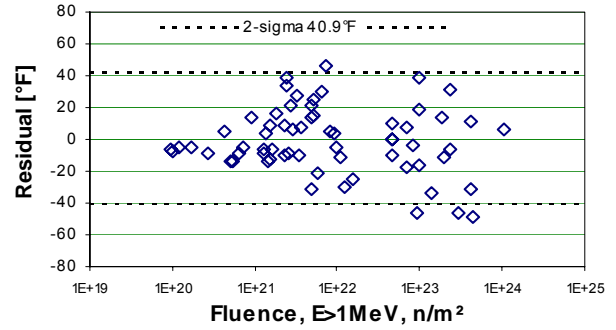


FIG. 11—Eason Model base residuals.

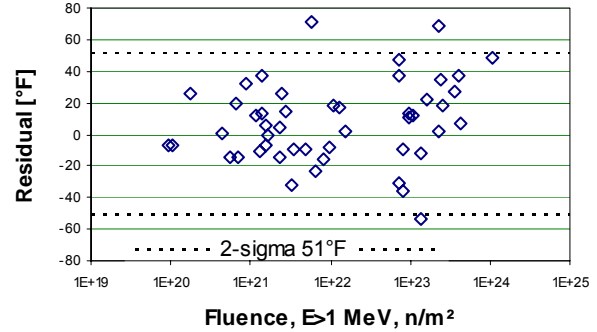


FIG. 12—Eason Model weld residuals.

the most common architecture. This architecture has additional layers of nodes between the input and output layers. The information from each input-layer node is fanned out to nodes in the layer hidden between the input and output layers. The information entering a node in any hidden or output layer is the weighted sum of all information leaving the layer below it in the hierarchy. The node performs a nonlinear/sigmoidal transformation on the weighted information it receives and fans out the result to all nodes in the layer above it in the hierarchy (except for the output layer). The weighting factors (weights) are free parameters that must be adjusted to some chosen criteria function using some optimization algorithm. In this way, ANNs are able to capture many higher-order correlations that may exist in the data. The relationship between the higher-order correlations produces a nonlinear mapping. This is the reason ANNs may offer a more accurate prediction of material behaviors, embrittlement in this case. Methods like ANNs provide a better tool to extract nonlinear relationships from embrittlement data to aid in the development of reliable maintenance and safety strategies and regulations in the nuclear industry.

The backpropagation algorithm is used to train the network with the data [20]. The training process determines the weights of ANNs to fit a suitable nonlinear map. The backpropagation's flexibility in training an ANN is why it does a better job of modeling than linear regression, but this method has several weaknesses. The backpropagation algorithm is based on local descent and can get stuck in local minima; as a result, the predictive properties can be quite varied. Also, there are a number of tunable parameters such as starting weights and learning rates that have a significant effect on the weight computed by the backpropagation algorithm. Thus, when different ANN models are trained with the same backpropagation algorithm but with different starting weights and learning rates,

ANN Models — An ANN is a parameterized nonlinear mapping from an input space to an output space [20]. An ANN realizes mapping from an m-dimensional input space to an n-dimensional output space and will have m nodes in its input layer and n nodes in its output layer. A multi-layer ANN (ML-ANN) is

the performance can be significantly different. These networks, however, can be fused to achieve the performance of the best ANN [4], creating a more robust architecture. Six independent variables, namely Cu, Ni, P, fluence, irradiation temperature, and effective full power time were used in the ANN models. A program written in C language was used in this study.

K-Nearest Neighbor Regression (K-NNR) Method — The NNR [6] is also chosen to generate an embrittlement model. The algorithm is described below. Let $x_1, x_2, x_3, \dots, x_n$ be a sequence of n independent measurements with known classifications, and x be the measurement to be classified. Among $x_1, x_2, x_3, \dots, x_n$ let the measurement with the smallest distance from x be denoted as x' . Then the nearest-neighbor decision rule assigns the classification of x' to that of x . As for K-NNR, it assigns to an unclassified sample point the class most heavily represented among its K nearest neighbors to x . In this study, we chose the first three nearest neighbors with properly weighted function to represent the unclassified sample.

Six independent variables, namely Cu, Ni, P, fluence, irradiation temperature, and effective full power time were used in K-NNR models. A second test K-NNR model, excluding irradiation temperature from the fitting parameter, generated a trend curve nearly identical to that with irradiation temperature. A program written in C language was used in this study.

Fusion of Embrittlement Models

The development of this model consists of identifying the error profiles of various estimators and the physical parameters of the underlying problem and designing the fusers for combining the individual estimators. Two types of information fusers were used in fuser model development, namely, linear fuser and near neighbor projective fuser.

Initially we combined the statistical and deterministic estimators using the linear fuser, which is a special case of the isolation fusers [21]. The isolation fusers are shown to perform probabilistically as well as best estimator [5,21]. Given n estimators, $f_1(x), \dots, f_n(x)$, the linear fuser is given by $f(x) = w_1 f_1(x) + \dots + w_n f_n(x)$, where $w_1 \dots w_n$ are the weights. We computed the weights for the fuser by minimizing the error of the fuser for the training set.

The projective fuser [9] based on the nearest neighbor concept was also implemented in the study. This fuser partitions the space of domain X into regions based on the nearest to the sample. For each region an estimator with the lowest empirical error is used to compute the function estimate for all points in the region. This fuser is easy to implement and provides finite-sample performance bounds under fairly general smoothness or non-smoothness conditions on the individual estimator.

The program was written in C where the solution is based on solving a quadratic programming problem. In this study, we utilized the linear fuser and near neighbor projective fuser to develop the embrittlement models; six parameters, namely Cu, Ni, P, fast fluence, irradiation time, and irradiation temperature, were incorporated into model development. Eight different models were investigated, including four neural network models, two ORNL models, the K-NNR method, and the Eason's model.

ORNL Fuser Model I — Linear Fuser was implemented into Fuser Model I development. The results of the linear fuser

model indicate that this newly developed embrittlement model results in about 56.5% and 32.8% reductions in uncertainties for GE BWR base and weld data, respectively, compared with the model of RG1.99/R2. These are substantial improvements on the embrittlement predictions for the RPV steels. The plots of information model residual and its two-sigma uncertainties for base and weld materials are illustrated in Figs. 13 and 14, respectively.

ORNL Fuser Model II — Fuser Model II is a simplified version of Fuser Model I, excluding the irradiation temperature from the fitting parameter and excluding Eason's model from the fusion modeling. The data scatter of residuals for Fuser Model II are essentially the same as that of Fuser Model I. The results of ORNL Fuser Model II indicate that it has about 55.2% and 28.8% reduction in uncertainties for GE BWR base and weld data, respectively, compared with the RG1.99/R2 model. This indicates that Fuser Model I has marginally improved performance with Fuser Model II. Thus, the impact of irradiation temperature on embrittlement modeling for the GE BWR surveillance data can be considered as secondary.

ORNL Fuser Model III — Nearest neighbor projective fuser was implemented in Fuser Model III development. The results of the projective fuser model indicate that it has about 67.3% and 52.4% reductions in uncertainties for GE BWR base and weld data, respectively, compared with that of RG1.99/R2. These are significant improvements in the embrittlement predictions for RPV steels. The plots of the information model residual and its two-sigma uncertainties for base and weld materials are illustrated in Figs. 15 and 16, respectively.

Discussion

The comparison of the performance of the embrittlement models, based on the two-sigma uncertainty of residual values, is stated in Table 1. The weights for the linear fuser models for base and weld data are illustrated in Table 2. Fuser Model III gave the best performance among all the embrittlement prediction models. ORNL embrittlement models indicate that ORNL Model II is superior to ORNL Model I because it includes irradiation time to simulate fluence-rate effect. Thus, the implication of a flux effect in BWR environment was revealed in the model development.

The authors would like to point out that the fusion modeling developed here is based on GE BWR data, including 112 available sample data, whereas, RG1.99/R2 and Eason's Model were developed based on both pressurized water reactor (PWR) and BWR surveillance data. Thus, the superior prediction by ORNL fusion models compared with RG1.99/R2 and Eason's models may be partially due to the subset of power reactor data used in the model development. However, by the same token, this study may also demonstrate the superiority and advantage of using subset data, for example, the vendor specific data, to develop power reactor embrittlement models. In general a large data set with similar characteristics or controllable parameters will generate a better trend prediction compared to its subset. But a misleading trend curve can result from a large data set built upon different bases and uncontrollable parameters, revealed by its large uncertainty.

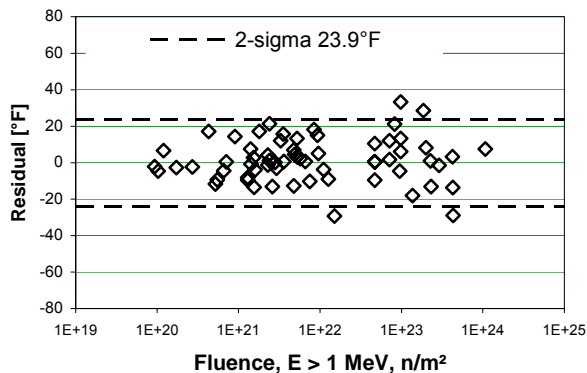


FIG. 13—Fuser Model I base residuals.

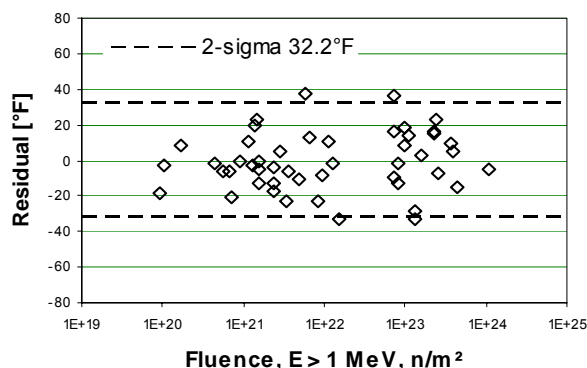


FIG. 14—Fuser Model I weld residuals.

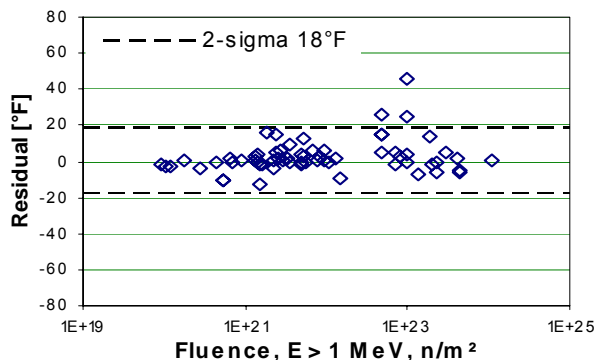


FIG. 15—Fuser Model III base residuals.

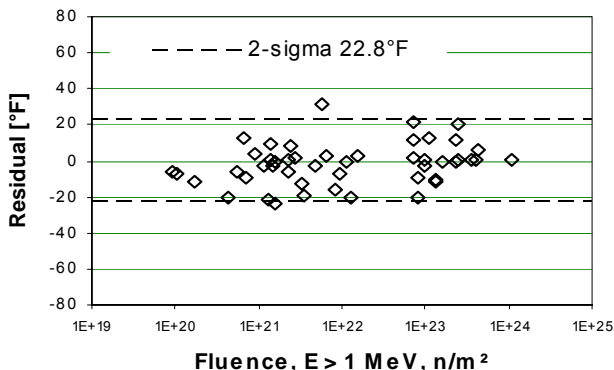


FIG. 16—Fuser Model III weld residuals.

Table 1—Two-sigma uncertainty of the embrittlement models for GE BWR data.

Embrittlement model	Parameters					Two sigma of residual (°F)	
	Cu	Ni	ϕt	t_i	T_c	Base (64 points)	Weld (48 points)
Reg. Guide 1.99, Rev. 2	x	x	x			55.0	47.9
ORNL Fuser I	x	x	x	x	x	23.9	32.2
ORNL Fuser II	x	x	x	x		24.6	34.1
ORNL Fuser III	x	x	x	x	x	18.0	22.8
ORNL Model I	x	x	x			39.6	41.8
ORNL Model II	x	x	x	x		27.6	38.5
Eason's Model	x	x	x	x	x	40.9	51.0
K-NNR Model	x	x	x	x	x	39.1	41.4
ANN-4 Model	x	x	x	x	x	56.4	78.8*

*| Residual | > 100°F are not included in two-sigma uncertainty evaluation.

Table 2—Optimized weights for ORNL linear fuser model.

Model	ANN1	ANN2	ANN3	ANN4	ORNL 1	ORNL 2	KNNR	Eason
Base	1.12	-0.15	0.28	-1.36	-0.068	0.693	0.661	-0.117
Weld	-0.62	0.073	0.86	-0.58	-0.050	0.800	0.502	0.0227

Regulatory Guide 1.99/R2 was formulated based on Guthrie's model and Odette's model and no temperature effect was considered in embrittlement model development; the fluence factor (FF) and the plates' chemistry factor (CF) are from Guthrie's model [18]. A total of 177 surveillance data were used in Guthrie's model development; however, only 6 data are from a BWR environment. Thus, BWR surveillance data may not be properly characterized from the RG1.99/R2 model. From the ASTM E10.02 database, the mean temperature and one standard deviation of BWR and PWR data are $540.3 \pm 13.6^\circ\text{F}$ and $545.7 \pm 10.4^\circ\text{F}$, respectively. Therefore, from the irradiation temperature variability point, the sample temperature environments of PWRs and BWRs are comparable. Currently, there are four major commercial power reactor vendors in the U.S., Westinghouse, General Electric, Babcock & Wilcox, and Combustion Engineering. Each vendor has its unique designs and specific operating procedures. There are significant problems associated with insufficient information, such as the detailed irradiation temperature of surveillance specimens, the thermal gradient within surveillance capsules, and the lack of data in particular regions of interest to characterize the vendor's service environments. About 64% of PR-EDB data is from Westinghouse; thus, the trend curve of all the four vendors' data will closely resemble the Westinghouse reactor environment. Furthermore, B&W surveillance data appear to experience higher irradiation temperature (based on capsule melting wire) than other vendors. Combining low- and high-temperature data may bring further bias on top of bias from the modeling point. For example, from the trend curve of all the vendor data, the high-irradiation-temperature data shows negative bias (i.e. A prediction model shows over-prediction) and low irradiation temperature data show positive bias. However, the overall biases (or uncertainties) will cancel each other, resulting in a misleading statistical outcome, such as means and uncertainty.

Eason's model covers both PWR and BWR environments, where 96 BWR data were included in model development and coolant inlet temperatures were incorporated into governing

equations to simulate temperature effect. In practice, the coolant inlet temperature is incorporated into the embrittlement model to simulate the irradiation temperature for a pressurized light-water reactor. However, a past study [11] showed that a large bias can still be identified in Eason's model for surveillance data from a higher-irradiation-temperature environment; and the bias is similar to that of RG1.99/R2 [18]. This may indicate that the coolant inlet temperature is not equivalent to the irradiation temperature experienced by the surveillance specimens. Furthermore, based on this study on fuser models, neither including nor excluding coolant inlet temperature has a significant impact on the trend curve, a finding that may further support the above statement.

For surveillance data, significant deviations of the measured shift from the trend curve (i.e., more or less than 34°F for plate materials) should be considered as a warning flag pointing to a possible anomalous capsule environment. The large uncertainties are the result of errors in the overall environment description. But, limited attention has been given to characterizing the irradiation temperature environment of the surveillance specimens. In general, the neutron environment, fluence and flux, can be determined fairly accurately; and possible effects from these sources are relatively small in a power reactor environment. However, the temperature of surveillance capsule environments still relies heavily on the measurement of the melting wire. A more detailed analytical investigation of specimen temperature is needed, based on detailed neutronic and thermal-mechanical analysis for specific capsule and specimen loading configuration, to facilitate the RPV surveillance program in confidence. Thus, in the current trend curve development, the most likely reason for deviations from the trend curve is the specimen temperature.

To develop a global embrittlement model for U.S. power reactors, an independent investigation of each subgroup (each vendor) is recommended. When the investigations are completed, if substantial improvement is achieved for each subset based on the proposed methodology, then an information fusion technique will be utilized to integrate all the subset models into a global RPV embrittlement model.

Conclusions

A new approach that incorporates chemical compositions into the Charpy trend curve was developed. The purpose of this new fitting procedure is to generate a new multi-space topography that can properly reflect the inhomogeneity of the surveillance materials and utilize this multi-space trend surface to link and project the surveillance test results to those for RPV steels. Furthermore, based on this new approach, the new advanced fitting procedure achieves a reduction in uncertainty by 27%, compared with the conventional hyperbolic tangent fit procedure.

We described an information fusion method for embrittlement prediction in light water RPVs by combining domain models with neural networks and NNs. Our method resulted in 67.3% and 52.4% reductions in 2-sigma uncertainties compared with the RG1.99/R2 model for base and weld materials, respectively. This new approach combines the conventional nonlinear methods and model-based methods into an integrated methodology applicable for modeling material aging processes. This approach can potentially assist the

nuclear industry on the issues of safety and lifetime extension of aging commercial nuclear power plants. By using a wide spectrum of methods, the proposed tool can potentially handle the subtle nonlinearities and imperfections and serve as a calibration and benchmark for the existing models. The predictions generated by our system have the potential for providing efficient, reliable, and fast results, and can be an essential part of the overall safety assessment of material aging research.

Future improvements of the proposed method can be achieved using the k -fold cross validation method [6]. In this method data is partitioned into k blocks, of which $k-1$ of them are used as the training set and the remaining as the test set. This process is repeated for all k permutations of choosing the $k-1$ blocks for the training set. Thus, at the end of this exercise, there are k accuracy estimates in terms of the average of test and training error. Using these k estimates we can compute the average accuracy, variance, and confidence interval. Based on the results, one can assign weights to various blocks in proportion to test error. These weights will then be used in developing an i -neighbor version of the proposed fuser. More generally, the cross validation method can also be used to compare various methods in a statistically informative manner.

Acknowledgments

This research is sponsored by the Laboratory Directed Research and Development Seed Money Program of Oak Ridge National Laboratory, and by the Engineering Research Program, Office of Basic Energy Sciences of the U.S. Department of Energy, under contract DE-AC05-00OR22725 with UT-Battelle, LLC.

REFERENCES

- [1] Wang, J. A., *Embrittlement Data Base, Version 1*, NUREG/CR-6506 (ORNL/TM-13327), U.S. Nuclear Regulatory Commission, August 1997.
- [2] Wang, J. A., *Analysis of the Irradiation Data for A302B and A533B Correlation Monitor Materials*, NUREG/CR-6413, ORNL/TM-13133, 1996.
- [3] Rao, N.S.V., "Multiple Sensor Fusion Under Unknown Distributions," *Journal of Franklin Institute*, vol. 336, no.2, pp. 285-299, 1999.
- [4] Rao, N.S.V., "Multisensor Fusion Under Unknown Distributions: Finite Sample Performance Guarantees," in *Multisensor Fusion*, A.K. Hyder (editor), Kluwer Academic Publishers, 2001.
- [5] Rao, N.S.V., "On Fusers That Perform Better Than Best Sensor," *IEEE Transactions on Pattern Analysis and Machine Intelligence*, vol. 23, no. 8, pp. 904-909, 2001.
- [6] Duda, R. O., Hart, P. E., and Stork, D. G., *Pattern Classification*, John Wiley and Sons, Second Edition, 2001.
- [7] Rao, N.S.V., Protopopescu, V., "On PAC Learning Of Functions With Smoothness Properties Using Feedforward Sigmoidal Networks," pp.1562-1569 in *Proceedings of IEEE*, vol. 84, no. 10, 1996.
- [8] Wang, J. A., "Development of Embrittlement Prediction Models for U.S. Power Reactors." pp.525-540 in *Effect of Radiation on Materials: 18th International Symposium*, ASTM STP 1325, March 1999.

- [9] Rao, N. S., "Nearest Neighbor Projective Fuser for Function estimation," *Proc. Conf. On Information Fusion*, 2002.
- [10] Mansur, L. K., "Mechanisms and Kinetics of Radiation Effects in Metals and Alloys," *Kinetics of Nohomogeneous Processes*, ed. by Gordon R. Freeman, 1987.
- [11] Wang, J. A., "Analysis of the Irradiated Data for A302B and A533B Correlation Monitor Materials," pp. 59-80 in *Effect of Radiation on Materials: 19th International Symposium*, ASTM STP 1366, ASTM, Philadelphia, March 2000.
- [12] Wang, J. A., Kam, F. B. K., and Stallmann, F. W., "Embrittlement Data Base (EDB) and Its Applications," *Effects of Radiation on Materials: Vol. 17*, ASTM STP 1270, pp. 500-521, August, 1996.
- [13] Guthrie, G. L., *Charpy Trend Curves Based on 177 PWR Data Points*, NUREG/CR-3391, U.S. Nuclear Regulatory Commission, 1983.
- [14] Odette, G. R., Lombrozo, P. M., Perrin, J. F., and Wullaert, R. A., *Physically Based Regression Correlations of Embrittlement Data From Reactor Pressure Vessel Surveillance Programs*, EPRI NP-3319, Electric Power Research Institute, 1984.
- [15] Fisher, S. B. and Buswell, J. T., *A Model for PWR Pressure Vessel Embrittlement*, Berkeley Nuclear Laboratories, Central Electric Generating Board, GL139PB, 1986.
- [16] Lowe, A. L. Jr., and Pegram, J. W., *Correlations for Predicting the Effects of Neutron Radiation on Linde 80 Submerged-Arc Welds*, BAW-1803, Rev. 1, May 1991.
- [17] Brillaud, C., Hedin, F., and Houssin, B., "A Comparison Between French Surveillance Program Results and Predictions of Irradiation Embrittlement," *Influence of Radiation on Material Properties*, ASTM STP 956, pp. 420-447, 1987.
- [18] Randall, P. N., "Basis for Revision 2 of the U.S. Nuclear Regulatory Commission's Regulatory Guide 199," *Radiation Embrittlement of Nuclear Reactor Pressure Vessel Steels: An International Review (Second Volume)*, ASTM STP 909, pp. 149-162, 1986.
- [19] Eason, E. D., Wright, J. E., and Odette, G. R., *Improved Embrittlement Correlations for Reactor Pressure Vessel Steels*, NUREG/CR-6551, U.S. Nuclear Regulatory Commission, 2000.
- [20] Hassoun, M. H., *Fundamentals of Artificial Neural Networks*, MIT Press, 1995.
- [21] Rao, N.S.V., "Finite Sample Performance Guarantees Of Fusers For Function Estimators," *Information Fusion*, vol. 1, no. 1, pp. 35-44, 2000.